1521-0111/99/6/460–468$35.00
MOLECULAR PHARMACOLOGY

https://doi.org/10.1124/molpharm.120.000180
Mol Pharmacol 99:460–468, June 2021

Identification of Chemical and Pharmacological Chaperones for Correction of Trafficking-Deficient Mutant Cyclic Nucleotide–Gated A3 Channels[S]

Joachim Täger,[1] Bernd Wissinger, Susanne Kohl, and Peggy Reuter

Molecular Genetics Laboratory, Institute for Ophthalmic Research (J.T., B.W., S.K., P.R.), and Graduate School of Cellular and Molecular Neuroscience (J.T.), University of Tübingen, Tübingen, Germany

Received October 4 2020; accepted March 30 2021

ABSTRACT

Trafficking deficiency caused by missense mutations is a well known phenomenon that occurs for mutant, misfolded proteins. Typically, the misfolded protein is retained by the protein quality-control system and degraded by the endoplasmic reticulum-associated protein degradation pathway and thus does not reach its destination, although residual function of the protein may be preserved. Chemical and pharmacological chaperones can improve the targeting of trafficking-deficient proteins and thus may be promising candidates for therapeutic applications. Here, we report the application of a cellular bioassay based on the bioluminescent calcium reporter aequorin to quantify surface expression of mutant CNGA3 channels associated with the autosomal recessively inherited retinal disease achromatopsia. A screening of 77 compounds enabled the identification of effective chemical and pharmacological chaperones that result in a 1.5- to 4.8-fold increase of surface expression of mutant CNGA3. Using selected compounds, we confirmed that the rescue of the defective trafficking is not limited to a single mutation in CNGA3. Active compounds and our structure-activity correlated data for the dihydropyridine compound class may provide valuable information for developing a treatment of the trafficking defect in achromatopsia.

SIGNIFICANCE STATEMENT

This study describes a novel luminescence-based assay to detect the surface expression of mutant trafficking-deficient CNGA3 channels based on the calcium-sensitive photoprotein aequorin. Using this assay for a compound screening, this study identifies novel chemical and pharmacological chaperones that restore the surface localization of mutant trafficking-deficient CNGA3 channels. The results from this work may serve as starting point for the development of potent compounds that rescue trafficking deficiencies in the autosomal recessively inherited retinal disease achromatopsia.

Introduction

Achromatopsia is a rare retinal disorder characterized by loss of cone photoreceptor function (Remmer et al., 2015). Six genes are associated with achromatopsia (Kohl et al., 1998, 2000, 2002, 2012, 2015; Chang et al., 2009): *CNGA3* (OMIM: 216900), *CNGB3* (OMIM: 262300), phosphodiesterase 6C (*PDE6C*, OMIM: 613093), phosphodiesterase 6H (*PDE6H*, OMIM: 610024), G protein subunit alpha transducin 2 (*GNAT2*, OMIM: 613856), and activating transcription factor 6 (*ATF6*, OMIM: 616517). Most patients carry mutations in *CNGA3* and *CNGB3* encoding for both subunits of the cyclic nucleotide–gated (CNG) channel expressed in the cone photoreceptor outer segment (Johnson et al., 2004). The cone CNG channel is a non-selective cation channel with a proposed stoichiometry of three CNGA3 and one CNGB3 subunit (Shuart et al., 2011). Both channel subunits are structurally homologous proteins consisting of six transmembrane helices (S1–S6), a pore region between S5 and S6, a ligand-binding domain for cyclic nucleotides (CNBD), and a C-linker connecting S6 with the CNBD. The main subunit is CNGA3, which can form functional homomeric channels in heterologous expression systems, whereas CNGB3 is the modulatory subunit (Kaupp and Seifert, 2002).

In earlier studies, we and others performed functional analysis of mutant homomeric and heteromeric cone CNG channels in heterologous expression systems (Faillace et al., 2004; Tränkner et al., 2004; Liu and Varnum, 2005; Nishiguchi et al., 2005; Patel et al., 2005; Muraki-Oda et al., 2007; Koeppen et al., 2008; Reuter et al., 2008; Ding et al., 2010; Koeppen et al., 2010; Matveev et al., 2010; Duricka et al.,

[1]Current affiliation: German Center for Neurodegenerative Diseases (DZNE), Tübingen, Germany.

The authors declare that they have no conflicts of interest with the contents of this article.

This work was supported by the Manchot Foundation, the German Federal Ministry for Research and Education [Grant 01GM1105A, IonNeurONet], and the Deutsche Forschungsgemeinschaft (DFG, German Research Foundation) [Grant 398539671 within the DFG-SPP 2127 research initiative].

https://doi.org/10.1124/molpharm.120.000180.

[S] This article has supplemental material available at molpharm.aspetjournals.org.

ABBREVIATIONS: 8-Br-cGMP, 8-bromoguanosine-3′,5′-cyclic monophosphate; CNG, cyclic nucleotide–gated; CNBD, Cyclic Nucleotide-Binding Domain; DHP, dihydropyridine; DPBS, Dulbecco's phosphate-buffered saline; FC, fold change; FCmax, FC of the compound concentration yielding the highest effect; HEK293, human embryonic kidney 293OMIM, Online Mendelian Inheritance in Man; RRID, Research Resource Identifier; TUDCA, Tauroursodeoxycholic Acid; WT, Wild-Type.

2012; Shaikh et al., 2015). Besides altered biophysical characteristics, pathogenic mutations were frequently shown to result in a reduced surface expression caused by a trafficking defect (Faillace et al., 2005; Tränkner et al., 2004; Liu and Varnum, 2005; Nishiguchi et al., 2005; Koeppen et al., 2008; Duricka et al., 2012; Shaikh et al., 2015). On the molecular level, the trafficking defect results from a protein folding deficit that is induced by the mutation (Conn and Janovick, 2009). During protein maturation, the misfolded protein is recognized and retained by the cellular protein quality-control system (Adams et al., 2019) and subsequently degraded. Trafficking defects have been identified frequently as a pathologic mechanism causing diseases (Tamarappoo and Verkman, 1998; Skach, 2000; Blom et al., 2003; Yam et al., 2005; Sato et al., 2009; Schaeffer et al., 2014; Kuech et al., 2016). However, in many cases, the mutant protein is still functioning and could execute its cellular function when reaching its intended subcellular location (Gelsthorpe et al., 2008). Thus, developing a strategy to avoid the mutant protein being trapped and degraded may result in a rescue of the disease phenotype.

Chemical chaperones reverse defective trafficking by either nonspecifically changing protein-solvent interactions, thus favoring correct folding (Leandro et al., 2008; Dandage et al., 2015), or increasing expression levels of heat shock proteins that support protein folding (Diamant et al., 2001). An elevated surface density of trafficking-deficient mutant CNGA3 has already been observed in cell culture systems after treatment with chemical chaperones (Koeppen et al., 2008; Duricka et al., 2012). However, the use of chemical chaperones for therapeutic applications is restricted because of their nonspecific effect on protein folding and the high concentrations needed.

Pharmacological chaperones are typically agonists or antagonists of the mutant protein and stabilize the target protein in its native conformation by direct binding (Leidenheimer and Ryder, 2014; Wang et al., 2014 b). Because of their specific interaction, effective concentrations lie in the low micromolar or nanomolar range, giving pharmacological chaperones a high potential for therapeutic purposes. The effectiveness of pharmacological chaperones is gaining traction, with a number of successful demonstrations of its use in recent years (Rigat and Mahuran, 2009; Dawson et al., 2010; Martin et al., 2013; Wang et al., 2014 a; Banning et al., 2016; Hoshina et al., 2018; Li et al., 2020). For trafficking-deficient cone CNG channels with mutations in the CNBD domain, it has been shown that treatment with an analog of the natural ligand cGMP results in an increased surface expression (Duricka et al., 2012).

In the present study, we identified substances that support proper folding and trafficking of mutant CNGA3 channels. An aequorin-based bioassay was established that enables a relative quantification of the CNGA3 channel density in the plasma membrane via CNGA3-mediated calcium influx. This assay was used to screen nine known chemical chaperones and 68 compounds—among them a substantial number of dihydropyridine (DHP) compounds. An additional 12 DHP derivatives were assayed to provide insights into structural requirements of DHP compounds for correction of the trafficking defect of mutant CNGA3 channels.

Materials and Methods

Plasmids. The generation of the wild-type and mutant human *CNGA3* (NM_001298.2) and *CNGB3* (NM_019098.4) expression constructs were described previously (Tränkner et al., 2004; Koeppen et al., 2008, 2010; Reuter et al., 2008). The plasmid pCAEQ, encoding for a mitochondrial localized apoaequorin, was kindly provided by Perkin Elmer (Waltham, MA) and was modified by excision of the mitochondrial targeting sequence. Cytoplasmic localization was confirmed by colocalization of the myc-tagged apoaequorin with the mitochondrial markers apoptosis-inducing factor (RRID: AB_726995) and Mitotracker Red CMXRos (Supplemental Fig. 1).

Cell Culture and Transfection. The human embryonic kidney 293 (HEK293, RRID: CVCL_0045) cells were maintained in high-glucose Dulbecco's modified Eagle's medium (Life Technologies Corporation, Carlsbad, CA) supplemented with 10% fetal calf serum (Life Technologies Corporation), 1% fungizone (Cytiva; Marlborough, MA), and 1% penicillin/streptomycin (Sigma-Aldrich GmbH, Munich, Germany) at 37°C and 5% CO_2. HEK293 cells were seeded at a density of approximately 2×10^5 cells/cm^2, and transfection was carried out using LipofectAMINE 2000 (Life Technologies Corporation). For bioassay and cell viability experiments, plasmids encoding for wild-type CNGA3 channels or $CNGA3_{E228K}$ channels and apoaequorin were cotransfected in a ratio of 1.0:2.1. For all remaining mutant CNG channels, a ratio of 1.0:0.3:2.1 for CNGA3, CNGB3, and apoaequorin was chosen. For Western blot experiments, HEK293 cells, at a confluence of 80%, were transfected with 7.5 μg plasmid DNA in a six-well plate.

At 6 hours post-transfection, HEK293 cells were washed with Dulbecco's phosphate-buffered saline (DPBS; Life Technologies Corporation), detached by treatment with trypsin-EDTA (Life Technologies Corporation), and seeded in opaque 96-well plates at a density of 7.5×10^4 cells per well for the aequorin-based bioassay and the cell viability experiments or 6-cm dishes for Western blot experiments. At 24 hours post-transfection, cells were treated with 3 mM sodium butyrate (Sigma-Aldrich GmbH) and the test compound over a duration of 24 hours. For any experiment, cells used for negative control, positive control, and treatment with a certain compound originated from the same transfection.

Aequorin-Based Bioassay. Cells were washed with DPBS and incubated with 8 μM coelenterazine (Biomol GmbH, Hamburg, Germany) in calcium imaging solution (5 mM KCl, 2 mM $CaCl_2$, 2 mM $MgCl_2$, 10 mM HEPES, 30 mM glucose, 150 mM NaCl, pH 7.4) for 4 hours to reconstitute the aequorin. Cells were washed with DPBS, and 90 μl of calcium imaging solution containing 10 mM $CaCl_2$ was added. Luminescence measurements were carried out using an Orion luminometer (Titertek-Berthold Detection Systems, Pforzheim, Germany) with a spectral range of 300–650 nm. Luminescence was recorded for 50 seconds, and 10 μl of 100 mM 8-bromoguanosine-3′,5′-cyclic monophosphate (8-Br-cGMP; BIOLOG Life Science Institute, Bremen, Germany) was applied 3 seconds after the measurement started. For data evaluation, the baseline luminescence before addition of the ligand 8-Br-cGMP (basal calcium flux) was subtracted for each measurement. The area under the curve was calculated for an interval of 26 seconds starting 8 seconds after application of the cGMP analog for cells expressing $CNGA3_{WT}$ or $CNGA3_{E228K}$ channels and a 26-second interval starting 16 seconds after ligand application for cells expressing other CNGA3 mutants. By this means, we only included the values corresponding to the peak of the calcium transient for analysis, excluding any application artifacts. For analyzing the data obtained by the compound screen, the fold change (FC) of the treated versus untreated cells or of wild-type versus mutant channels was determined.

Screening and Experiments with Wild-Type and Additional Mutant CNGA3 Channels. To evaluate the effect of chaperone treatment, solvent-treated cells (designated as untreated control throughout the document) were used as control. Treatment with 2.5% glycerol served as a positive control for cells expressing wild-type or mutant CNG channels. Concentrations of chemical chaperones ranged between 0.5 and 850 mM. Ion channel antagonists and their derivatives were first screened in quadruplicate using 3.3, 10, 33, and 100 μM of the compounds. Compounds showing an FC of about 1.0 at all tested concentrations were retested at higher concentrations, whereas compounds showing an FC smaller than 1.0 at all

concentrations, indicating toxicity of the compound, were retested at lower concentrations. To classify compounds as active, we defined an arbitrary FC cutoff value of 1.5. Activity of compounds was confirmed in two independent experiments using six concentrations close to the estimated signal maximum. The follow-up experiments using wild-type and additional trafficking-deficient CNGA3 were done in quadruplicate and in two independent experiments.

Cell Viability Assay. Compounds were tested in their most effective concentration, which was determined by the bioassay. After compound treatment, cells were washed with DPBS, and 50 μl of calcium imaging solution was added to the wells. Subsequently, the CellTiter-Glo Luminescent Cell Viability Assay (Promega GmbH, Mannheim, Germany) was performed following the manufacturer's instructions using the Orion luminometer. Two independently transfected cell populations were tested in quadruplicate, and statistical analysis was performed, as described below.

SDS-PAGE and Western Blot Experiments. Cells were trypsinized, washed gently with DPBS buffer, and transferred into ice-cold lysis buffer (1 mM Dithiothreitol, 1 mM EDTA, 50 mM Tris, and 150 mM NaCl, pH 7.4) containing 1% proteinase inhibitor cocktail (Merck Millipore, Billerica, MA). Cell lysis was performed by four freeze/thaw cycles using liquid nitrogen. After cell debris removal by centrifugation at 500x*g* for 10 minutes at 4°C, membrane fractions were enriched by centrifugation at 30,000x*g* for 45 minutes at 4°C. Pellets were resuspended in 50 μl lysis buffer containing 1% NP40 and 0.25% sodium deoxycholate, and the protein concentration was determined using Bradford assay. Total protein lysates were incubated with Laemmli buffer (60 mM Tris-HCl, 10% glycerol, 5% 2-mercaptoethanol, 2% SDS, 0.01% bromophenol blue) for 1 hour at 4°C. Samples were separated on a 10% SDS-polyacrylamide gel. After transfer onto nitrocellulose membranes, blots were blocked overnight with 5% milk powder (Bio-Rad Laboratories GmbH, Munich, Germany) in Tris-buffered saline supplemented with 0.1% Tween 20 and probed with a mouse anti–myc-tag antibody (1:700; RRID: AB_10541551; Enzo Life Sciences, Lörrach, Germany) for the detection of apoaequorin, and the custom-made rabbit anti-CNGA3 antibody SA3899. The mouse anti–β-actin antibody staining (1:4000; RRID: AB_2223041; Merck Millipore) served as a loading control. For detection, horseradish peroxidase–conjugated goat anti-mouse (1:10 000; RRID: AB_437779; Merck Millipore) and horseradish peroxidase-conjugated donkey anti-rabbit (1:4000; RRID: AB_772206; GE Healthcare Life Sciences, Freiburg, Germany) secondary antibodies were used. Protein bands were quantified using ImageJ (RRID: SCR_001935; National Institutes of Health, Bethesda, MD).

Statistical Data Analysis. For statistical analysis of the bioassay results, the FC of treated samples versus untreated controls was calculated. For bioassay experiments and the quantification of the Western blots, fold changes are depicted as means and 95% confidence intervals throughout the whole document. For the cell viability assay, the viability of the untreated cells was set to 100%, and treated samples referred to that. Box plots are shown as median and upper as well as lower quartile. The whiskers represent the maximum and minimum value for each data set. Statistical analysis was performed using the Mann-Whitney *U* test for pairwise comparison of each compound treatment with the untreated control using Mystat (Systat Software Inc., London, UK), and the Kruskal-Wallis one-way ANOVA with the Dunn's post hoc test was applied for multiple comparison (GraphPad Prism, San Diego). Statistical significance of the data was defined as follows: $*P < 0.05$; $**P < 0.01$; and $***P < 0.001$. This study is exploratory by nature.

Results

Identification of Compounds Increasing the Luminescence Signal in the Bioassay and Effect of the Six Most Potent Compounds on Cell Viability. Homomeric CNGA3 channels are integrated into the plasma membrane of transfected HEK293 cells and conduct ions along their concentration gradient after addition of the CNG channel ligand 8-Br-cGMP. This calcium flux can be monitored using the genetically encoded calcium-sensitive photoprotein aequorin, which resides in the cytoplasm. The ligand-induced calcium flux results in a strong increase of the luminescence that is absent in cells not expressing CNG channels and thus solely represents CNG channel–mediated calcium flux, as shown previously (Täger et al., 2018) and in Supplemental Fig. 2. Using this luminescence-based bioassay, we performed a screening of nine known chemical chaperones and 65 ion channel antagonists and three DHP derivatives for their potential to increase the luminescence signal compared with the untreated control. The ion channel antagonists were selected manually based on known interaction with CNGA3 or other cation channels and their commercial availability.

For the screening, CNGA3 channels with the mutation p.E228K, which is located in the intracellular loop connecting S2 and S3, were used. The mutation p.E228K is primarily impaired by a trafficking defect since the apparent ligand sensitivity was found to be similar to wild-type channels (Reuter et al., 2008). Also, the impact of the mutation p.E228K onto CNG channel functionality is rather mild since $CNGA3_{E228K}$ channels conduct ions, as observed by electrophysiology (Reuter et al., 2008) and the bioassay described here (Täger et al., 2018). Because of this residual activity, toxic side effects of compounds were detected. As a positive control throughout the screening, we used glycerol, which has already been shown to possess a beneficial effect on surface expression of mutant CNGA3 channels (Koeppen et al., 2008). A table showing all compounds and the results of the bioassay is available in the supporting information (Supplemental Table 1).

To only classify medium and strong compound effects as active, we considered compounds reaching an FC of 1.5 or higher as active. The screening was performed using initially four concentrations of the test compounds. If compound activity was observed, the compound was retested twice with six concentrations. If the compound treatment caused toxicity, lower concentrations were tested, and if the FC of all tested concentrations did not deviate from 1.0, higher concentrations were used. Typically, only the FC of the compound concentration yielding the highest effect is presented (FC_{max}).

Of the nine chemical chaperones tested, only L-glutamine at a concentration of 100 mM showed activity resulting in an FC_{max} of 1.5 ± 0.2 (Fig. 1A). The other chemical chaperones did not show activity. Based on their molecular structure, the ion channel antagonists tested were subdivided into several classes. Of those, the largest class, consisting of 17 compounds, was the DHP class, which inhibits preferentially L-type calcium channels. Eight of the DHPs (47%) were active possessing an $FC_{max} \geq 1.5$, and of those, nisoldipine had the highest effect, with an FC_{max} of 4.8 ± 0.7 at 20 μM (Fig. 1A). The effect of 15 μM JFD03311, having an FC_{max} of 2.4 ± 0.1, is considerably lower compared with nisoldipine. The other six active DHPs had FC_{max} values between 1.5 and 2.0. The lowest concentration necessary to reach FC_{max} was obtained after treatment with 0.66 μM niguldipine (FC_{max} of 1.6 ± 0.1).

Another class of pharmacological chaperones comprised five pyrazin amides and benzamides, which were shown to be active, with FC_{max} between 1.5 ± 0.1 (10 μM cisapride) and 3.8 ± 0.6 (400 μM amiloride). Of the remaining 46

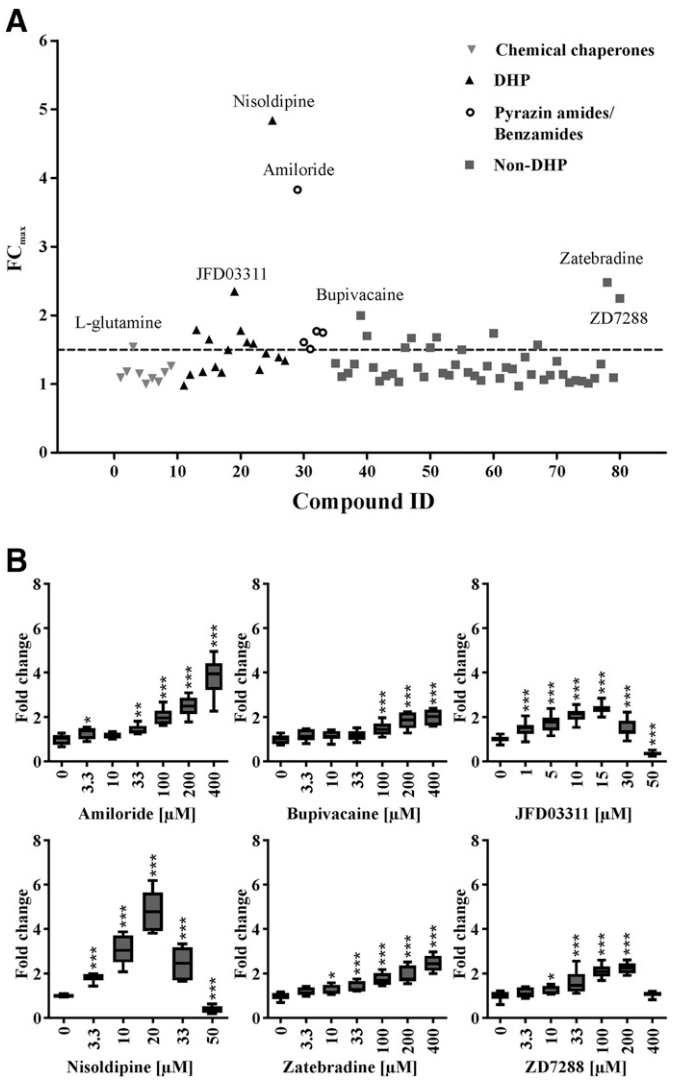

Fig. 1. Result of compound screening. (A) HEK293 cells expressing the reconstituted calcium sensor aequorin and the mutant $CNGA3_{E228K}$ channel were used for the screening. Treatment with nine known chemical chaperones, 17 DHPs, five pyrazin amides/benzamides, and 46 non-DHPs was carried out to identify active chemical and pharmacological chaperones for mutant CNGA3 channels. The fold change represents the calcium signal obtained by treatment with the most efficient compound concentration (FC_{max}) divided by the calcium signal obtained for the untreated control. To be classified as "active," compounds needed to show an FC_{max} of ≥1.5 and a P value of <0.05. Supplemental Table 1 gives an overview of the results for each compound measured with this bioassay. (B) Shown is a graphical representation of dose-response curves for the six identified best hits: amiloride, bupivacaine, JFD03311, nisoldipine, zatebradine, and ZD7288 ($n \geq 4$; $^*P < 0.05$; $^{**}P < 0.01$; $^{***}P < 0.001$).

non-DHPs, 11 compounds (24%) showed activity. Among them were the *N*-phenylsulfonamide zatebradine, a hyperpolarization-activated cyclic nucleotide–gated channel antagonist, with an FC_{max} of 2.5 ± 0.2 at 400 μM, and the human ether-a-go-go–related gene potassium channel antagonist E-4031, a high-molecular-weight compound containing dimethoxybenzene groups, with an FC_{max} of 1.7 ± 0.2 also at 400 μM. Additionally, the hyperpolarization-activated cyclic nucleotide–gated channel antagonist ZD7288 and the voltage-gated sodium channel antagonist bupivacaine were identified as active hits, with ZD7288 having an FC_{max} of 2.2 ± 0.1 at 200 μM and bupivacaine having an FC_{max} of 2.0 ± 0.2 at 400 μM.

The dose-dependent effects of the six compounds with highest FC_{max} (nisoldipine, JFD03311, amiloride, zatebradine, ZD7288, and bupivacaine, with $FC_{max} \geq 2.0$) are plotted in Fig. 1B. With the exception of nisoldipine, we observed a moderate increase in FC with increasing compound concentration until reaching FC_{max}. In the case of amiloride, bupivacaine, and zatebradine, the concentration eliciting the maximum FC was the highest concentration tested, whereas for JFD03311 and ZD7288, the luminescence signal decreased after reaching FC_{max}. In contrast, nisoldipine showed a rapid increase and decline in FC in a concentration range that is much smaller than for the other compounds. It is also striking that the concentrations needed to reach FC_{max} are lower for the DHPs nisoldipine and JFD03311 compared with the non-DHPs.

The six compounds with highest FC_{max} were further evaluated by testing for toxic side effects at their most effective concentration using a luminescence-based cell viability assay. Neither JFD03311 nor amiloride affected cell viability, whereas treatment with nisoldipine, zatebradine, or bupivacaine caused a reduction of cell viability by 10%–20%, with $P < 0.001$. However, the strongest effect was observed after treatment with ZD7288, which reduced cell viability by more than 30% (Fig. 2).

Effect of Pharmacological Chaperones onto the Expression of $CNGA3_{E228K}$ and Apoaequorin. We performed follow-up experiments to confirm that the observed increase in the luminescence signal after compound treatment indeed is a result of improved CNG channel trafficking. For that purpose, cells treated with the six compounds at the concentration yielding the highest FC_{max} were subjected to Western blot experiments to analyze the expression levels of $CNGA3_{E228K}$ and the reporter apoaequorin. We observed that treatment of cells with glycerol, zatebradine, and ZD7288 caused a 2-fold increase in the expression level of apoaequorin: JFD03311 provoked a

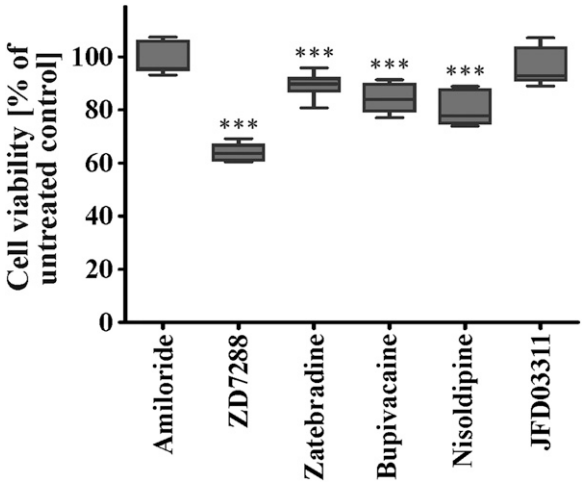

Fig. 2. Analysis of cell viability after compound treatment. HEK293 cells were treated with amiloride, ZD7288, zatebradine, bupivacaine, nisoldipine, and JFD03311 at their most effective concentration. Cell viability was determined by measuring total ATP content per well ($n = 8$; $^{***}P < 0.001$).

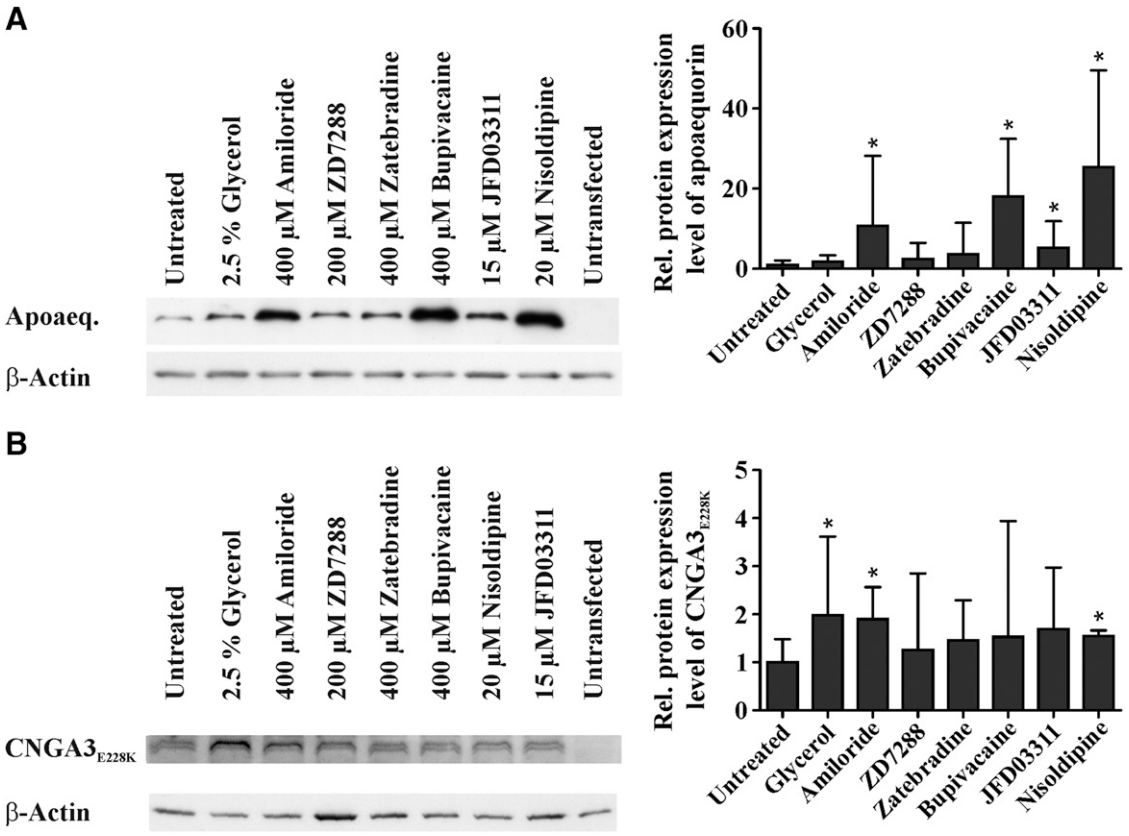

Fig. 3. Investigation of effects of compound treatment on apoaequorin and $CNGA3_{E228K}$ expression levels. HEK293 cells expressing either (A) apoaequorin or (B) $CNGA3_{E228K}$ were treated with the compounds that showed the highest effects in the primary screen at their most effective concentrations. Glycerol being the positive control in the screening procedure was included as well. Expression levels were quantified using membrane-enriched fractions of three replicates per treatment (Rel.: Relative; $^*P < 0.05$; data are represented as means ± 95% confidence interval).

5-fold increase ($P < 0.05$), and amiloride, bupivacaine, and nisoldipine induced a 10- to 25-fold increase ($P < 0.05$) in apoaequorin expression (Fig. 3A). Expression levels of $CNGA3_{E228K}$ were also increased after treatment with all compounds; however, the effects were milder compared with apoaequorin, with a 1.5- to 2.0-fold increase of $CNGA3_{E228K}$ (Fig. 3B). Thus, the high FC_{max} observed for some compounds in the bioassay using $CNGA3_{E228K}$ may have been caused, at least partially, by affecting the expression levels of $CNGA3_{E228K}$ and apoaequorin.

To evaluate the effect of the overexpression on the bioassay signals, we used cells expressing the wild-type CNGA3 channel, which is not impaired by a trafficking defect. Any increase in the luminescence therefore would reflect the effect of CNGA3 and apoaequorin overexpression. For this experiment, we focused on nisoldipine, amiloride, bupivacaine, and JFD03311, which all showed at least a 5-fold increase in apoaequorin levels. Nisoldipine (FC = 2.7 ± 0.1), amiloride (FC = 2.1 ± 0.2), and bupivacaine (FC = 1.9 ± 0.1) treatment indeed caused a strong increase of the luminescence signal after treatment of $CNGA3_{WT}$, correlating with the higher apoaequorin expression observed in the Western blot experiments (Fig. 4). This increase was not present after treatment with JFD03311. To verify that—despite the overexpression effects—a rescue of $CNGA3_{E228K}$ channel trafficking is conferred by compound treatment, we compared the fold changes obtained with $CNGA3_{E228K}$ and $CNGA3_{WT}$. Luminescence signals after treatment of $CNGA_{E228K}$ with nisoldipine, amiloride, or JFD03311 were at least >1.7-fold higher ($P < 0.001$) compared with treatment of $CNGA3_{WT}$. No difference was observed after treatment of $CNGA3_{WT}$ or $CNGA3_{E228K}$ with bupivacaine (Fig. 4). Thus, we confirmed that the overexpression effect is not the major reason for hit identification of DHP compounds in the luminescence-based assay. Furthermore, we showed that no or only a minor overexpression effect was observed for five additional hits from the screening (Supplemental Fig. 3).

Rescue of Other Trafficking-Deficient CNGA3 Channels. Typically, pharmacological chaperones are able to correct the folding and trafficking defect caused by different mutations in the protein of interest (Wu et al., 2011; Wang et al., 2014a). To test this hypothesis, we treated cells expressing trafficking-deficient CNGA3 channels carrying missense mutations in S4 (p.R283Q, p.T291R), the pore-forming domain (p.S341P, p.E376K), the linker (p.R427C), and the ligand-binding domain (p.R563C) with amiloride, JFD03311, nisoldipine, zatebradine, and ZD7288 at their most effective concentrations, which were identified in the initial screening using $CNGA3_{E228K}$ (Table 1). For simplification, we only show the corrected fold change for each treatment based on the experiment using wild-type CNGA3.

Amiloride was able to rescue the trafficking defect of all mutant CNGA3 channels, whereas the rescue effect of ZD7288 and zatebradine was limited to mutations located in S4 and the pore-forming region. Treatment with the DHP nisoldipine was able to correct the misfolding of $CNGA3_{T291R}$ and $CNGA3_{S341P}$ but also resulted in low or even negative FC for three out

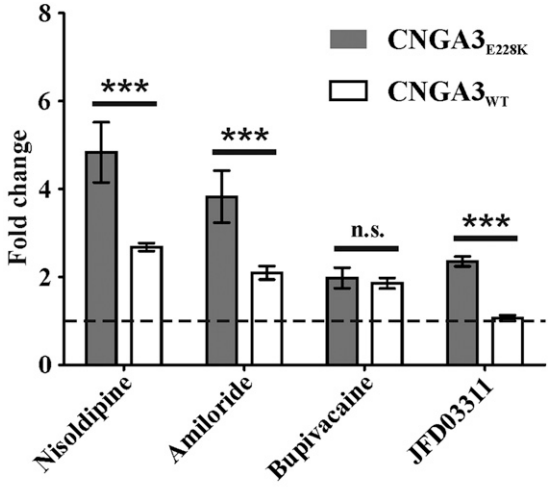

Compound	Conc. [μM]	FC for $CNGA3_{E228K}$	FC for $CNGA3_{WT}$
Nisoldipine	20	4.8 ± 0.7	2.7 ± 0.1
Amiloride	400	3.8 ± 0.6	2.1 ± 0.2
Bupivacaine	400	2.0 ± 0.2	1.9 ± 0.1
JFD03311	15	2.4 ± 0.1	1.1 ± 0.1

Fig. 4. Effect of compound treatment on the wild-type CNGA3-mediated bioassay signal. $CNGA3_{WT}$ is not affected by a trafficking defect. HEK293 cells expressing $CNGA3_{WT}$ channels were used to measure increases in bioassay signal, which are caused by unspecific effects due to compound treatment, and the resulting fold changes compared with the values obtained by using $CNGA3_{E228K}$-expressing cells. For nisoldipine and amiloride, the fold change obtained by using the mutant CNGA3 channel is still statistically significantly higher (Conc.: Concentration; $n = 8$; $^{**}P < 0.01$; $^{***}P < 0.001$; data are represented as means ± 95% confidence interval). The data are summarized in the table below.

of four of the remaining CNGA3 channel mutants tested. JFD03311 corrected the misfolding of both S4 channel mutants, $CNGA3_{S341P}$ and $CNGA3_{R427C}$. The highest FC were observed for amiloride and ZD7288 when expressing $CNGA3_{S341P}$ channels, with values of 5.0 ± 0.4 and 3.7 ± 0.3, respectively.

Analysis of Structural Features Improving DHP Activity. Since many compounds analyzed in this study belong to the dihydropyridine class of compounds, and additional derivatives were commercially available, we aimed to investigate the structure-activity relationship of the DHP. For that purpose, 12 additional DHPs with distinct modifications at R_1 to R_3 of the dihydropyridine backbone were included (Fig. 5A). A summary of the FC_{max} obtained for all 28 tested DHPs is shown in Supplemental Table 2. The structural features of these DHP derivatives are summarized in Supplemental Table 3.

In Fig. 5B, we give an overview of all compound classes tested, which includes compounds with modification on the benzene ring, the dihydropyridine ring, and at the dihydropyridine nitrogen on FC_{max}. The modifications on the benzene ring were subdivided into three categories. Many of the DHPs harbor a nitro group at the benzene ring, which may serve as an electron acceptor for the interaction with mutant CNGA3 channels. Others carry an unmodified or a halogen-substituted benzene ring or, alternatively, a large polar residue at the benzene ring.

To understand which of the compound modifications is important for the interaction with $CNGA3_{E228K}$, a comparison of the FC_{max} of the DHP groups was performed. With the exception of the DHPs sharing an unmodified or a halogen-substituted benzene ring (average FC_{max} = 1.2), all other compound classes yielded an FC_{max} of 1.5 or higher. The highest effects yielded DHP with a nitro group at the benzene ring with an average FC_{max} of 2.0 in the bioassay. We performed an ANOVA analysis and could show that the analyzed compound groups possess statistically significant differences among groups (P = 0.006). DHPs having a nitro group at the benzene ring exhibited a 1.7-fold higher FC_{max} ($P < 0.05$) compared with unmodified or halogen-substituted DHPs, indicating that a nitro group at R_1 is beneficial for their interaction with $CNGA3_{E228K}$. Adding a larger substituent at the dihydropyridine nitrogen at R_3 also increased FC_{max} by a factor of 1.6 ($P < 0.05$) compared with the unmodified or halogen-substituted DHPs. Modifications at the dihydropyridine ring, such as altered ester side chain modifications or the presence of an oxocyclohexene ring, had only minor effects on FC_{max}. In summary, addition of a nitro group at the benzene ring or adding residues at the dihydropyridine nitrogen represents an efficient strategy to increase the effect of compounds on mutant $CNGA3_{E228K}$ channels.

Discussion

This study aimed to identify chemical and pharmacological chaperones that correct the trafficking defect of mutant CNGA3 channels. To establish a robust assay for screening, we used a functional readout based on the CNGA3 channel–mediated calcium influx. This enabled the indirect quantification of CNGA3 channels localized in the plasma membrane. HEK293 cells do not express endogenous CNG

TABLE 1

Effect of compound treatment on additional mutant CNGA3 channels.HEK293 cells expressing reconstituted aequorin and heteromeric trafficking-deficient CNGA3 channels with mutations in transmembrane helix S4 (p.R283Q, p.T291R), the pore-forming region (p.S341P, p.E376K), the linker (p.R427C), or the ligand-binding domain (p.R563C) were treated with 400 μM amiloride, 200 μM ZD7288, 200 μM zatebradine, 20 μM nisoldipine, or 15 μM JFD03311. FC of treated vs. untreated samples are shown ($n = 8$; data are represented as means ± 95% confidence interval).

	Amiloride	ZD7288	Zatebradine	Nisoldipine	JFD03311
$CNGA3_{R283Q}$	2.3 ± 0.5a	2.2 ± 0.4a	1.8 ± 0.4a	0.3 ± 0.4	1.6 ± 0.3a
$CNGA3_{T291R}$	2.0 ± 0.2a	2.1 ± 0.1a	1.5 ± 0.1a	1.6 ± 0.5a	1.7 ± 0.3a
$CNGA3_{S341P}$	5.0 ± 0.4a	3.7 ± 0.3a	2.0 ± 0.2a	1.7 ± 0.3a	1.9 ± 0.2a
$CNGA3_{E376K}$	2.1 ± 0.6a	1.5 ± 0.1a	1.7 ± 0.1a	1.1 ± 0.3	1.2 ± 0.1
$CNGA3_{R427C}$	1.5 ± 0.5a	1.1 ± 0.2	1.4 ± 0.3	0.6 ± 0.6	1.8 ± 0.5a
$CNGA3_{R563C}$	1.9 ± 0.2a	1.2 ± 0.1	1.3 ± 0.1	−0.5 ± 0.3	1.1 ± 0.1

[a]Results with FC ≥ 1.5 were considered as active.

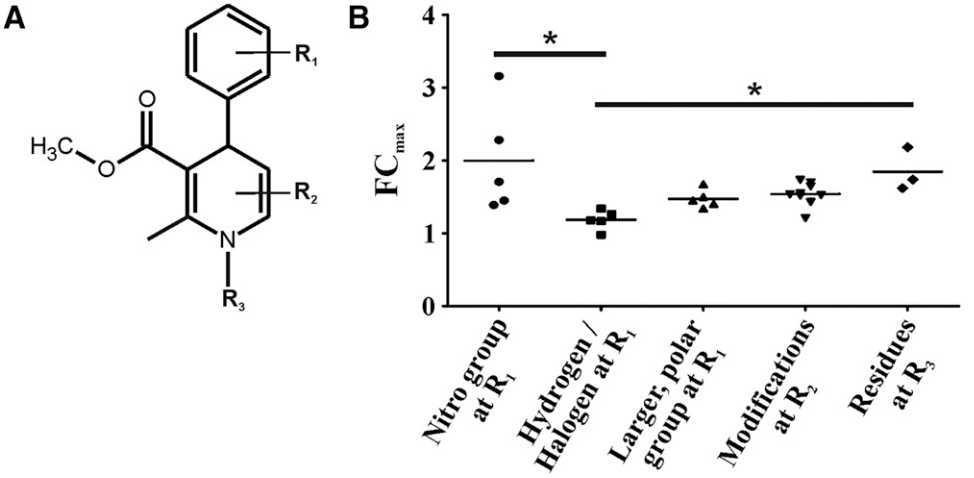

Fig. 5. Determining structural requirements of DHPs for improving $CNGA3_{E228K}$ interaction. The effect of DHP with certain structural features was evaluated on HEK293 cells expressing aequorin and $CNGA3_{E228K}$. (A) Representation of common structural features of DHP compounds and location of modifications on residues R_1–R_3, as described in (B). (B) Effects of DHP modifications on R_1–R_3 on FC_{max}. Statistical analysis showed that DHP with a nitrobenzene group and DHP with larger substitutions at the dihydropyridine nitrogen possess higher FC_{max} than DHP with unmodified or halogen-substituted benzene rings ($n \geq 4$; Kruskal-Wallis one-way analysis of variance, $P = 0.006$; Dunn's Post hoc test, $^*P < 0.05$).

channels or other cyclic nucleotide–activated calcium channels. Thus, the strong calcium signal elucidated by the application of 8-Br-cGMP in our bioassay solely represented the function of the transiently expressed CNGA3 channels (Supplemental Fig. 2). For relative calcium quantification, the genetically encoded calcium sensor aequorin was used, allowing the detection of calcium exclusively in the cell cytoplasm, thus minimizing background signal (Brini, 2008). The bioluminescent aequorin has been used previously for assay development and screening (Menon et al., 2008; Haq et al., 2013; Arduino et al., 2017).

For compound screening, the FC of the calcium signal obtained in the treated condition versus the calcium signal of an untreated control was calculated. We defined compounds as active when yielding a P value of <0.05 and an FC cutoff value of $\geq$1.5-fold. This allowed the identification of strong hits and the removal of hits with minor effects (Fig. 1). The screening of 77 compounds resulted in the identification of 22 chemical and pharmacological chaperones (hit rate: 29%). Compared with other screening campaigns, this hit rate is extremely high (Nühs et al., 2015; Atzmon et al., 2018; Stevens et al., 2019), but it can be explained by the following: 1) we specifically selected known ion channel antagonists for the screening, 2) a large number of active compounds were structurally related, and 3) we tested each compound in a broad concentration range with four to six compound concentrations.

By testing nine selected chemical chaperones, we identified L-glutamine as a hit. The activity of L-glutamine may rely on its ability to enhance the expression of the stress-inducible heat shock protein 70 (Moura et al., 2018), and increased amounts of this protein have already been shown to reduce protein misfolding (Choo-Kang and Zeitlin, 2001; Young, 2014). Another chemical chaperone tested was TUDCA, which has been reported to increase surface localization of heteromeric CNG channels with the mutations p.R563C and p.Q655X in CNGA3 (Duricka et al., 2012). Although we obtained a statistically significant increase in the FC of 1.3 after treatment with 3.3 mM TUDCA, indicating an increased surface localization of $CNGA3_{E228K}$, TUDCA was classified as inactive as a result of our stringent hit selection criteria.

For many screening campaigns, the hits identified in primary screening projects cannot be replicated. This may be due to false-positive hits caused by the experimental settings or compound properties (Gilberg et al., 2016; Horvath et al., 2016; Jasial et al., 2017). In this regard, we can exclude that the compounds studied here had effects on the biophysical properties of the CNGA3 channel, since compounds were washed out before performing the functional assay. By subtraction of the baseline signal from each measurement before analyzing the calcium signal, we can rule out any effects of changes in the basal calcium levels on our analysis. Additionally, we investigated the validity of the results obtained for the six best hits by analyzing whether these compounds altered the expression of $CNGA3_{E228K}$ or apoaequorin (Fig. 3). Indeed, we observed for amiloride, bupivacaine, JFD03311, and nisoldipine an increased abundance of apoaequorin in Western blot experiments. This might be a result of elevated transcription/translation, increased protein stability, or interference with degradation of apoaequorin. Interestingly, the effect onto $CNGA3_{E228K}$ abundance was milder: a 1.3- to 2-fold increase was observed for all compounds; however, statistically significant effects were only present after treatment with amiloride and JFD03311.

To study how this effect would affect the luminescence signal, we repeated the compound treatment and bioassay using wild-type CNGA3 channels that do not have a trafficking defect. We saw an increase in fold change after treatment with amiloride, JFD03311, nisoldipine, and bupivacaine. However, for amiloride, JFD03311, and nisoldipine, the FC obtained using $CNGA3_{E228K}$ channels was $>$1.5-fold higher than that of wild-type CNGA3-expressing cells, suggesting that besides the overexpression effect, these compounds also improved surface trafficking of the mutant channel. This was not true for bupivacaine, indicating that this compound represents a false-positive hit.

Using additional mutant CNGA3 channels, we confirmed that the identified compounds can also correct the trafficking defect induced by the mutations p.R283Q, p.T291R, p.S341P, p.E376K, p.R427C, and p.R563C (Table 1). Since $CNGA3_{S341P}$ and $CNGA3_{E376K}$ channels have previously been shown to be only functional in the presence of the CNGB3 subunit (Koeppen et al., 2010), we assayed all test compounds using cells

expressing heteromeric CNG channels. For most of the five compounds, an improvement of the trafficking of CNGA3 channels with mutations in the transmembrane helices or the pore-forming region was observed. This is not surprising since many of the tested antagonists interact with residues at the extracellular site or close to the center of the pore of the respective ion channels (Nakayama and Kuniyasu, 1996; Kamiya et al., 2008, Catterall and Swanson, 2015; Tanguay et al., 2019), and we propose that this is also the side of interaction with the CNGA3 channel for most of the tested compounds. Amiloride was shown to bind to the epithelial sodium channel in a region close to the pore (Schild et al., 1997). Thus, it is surprising that amiloride was able to rescue $CNGA3_{R563C}$ channels. Since this mutation is located in CNBD, we speculate that amiloride may have a second binding site close to this mutation. Overall, we confirmed that pharmacological chaperones were able to rescue several different mutant CNGA3 channels in the presence of the CNGB3 subunit—an observation that may also be important with respect to therapeutic applications.

Correcting the surface expression of trafficking-deficient ion channels is only possible when the compound enters the cell to bind to the mutant ion channel. Since many ion channel antagonists bind extracellularly to the ion channel, modification of compound structures to increase membrane permeability and specificity are inevitable. We first undertook experiments to elucidate the functional groups that are essential for interaction of DHP compounds with $CNGA3_{E228K}$ (Fig. 5). We could show that the nitrophenyl group is essential for efficiency of DHP, and larger, polar substitutions at the DHP nitrogen yielded >1.6-fold higher FC_{max} compared with DHP with unmodified or halogen-substituted benzene rings. Similar to our study, the identification of structural features of DHP important for antagonizing N-type calcium channels (Yamamoto et al., 2008) or the potentiation of the cystic fibrosis transmembrane conductance regulator (Pedemonte et al., 2007) were reported. In both studies, halogenated phenyl rings yielded better effects than nitrophenyl groups, indicating that this feature is important for the specific interaction with CNGA3 channels.

ZD7288 yielded an FC_{max} of 2.2 ± 0.1 at a concentration of 200 μM. However, we observed high toxicity in the cell viability assay (Fig. 2), resulting in a loss of about 30% of the cells, which is also reflected in the bioassay experiments using wild-type CNGA3. Therefore, the effect of ZD7288 seems to be specific and is underestimated because of its toxicity. Amiloride at 400 μM yielded the highest fold increase measured with the bioassay when using $CNGA3_{S241P}$ channels (FC of 5.0 ± 0.4). Despite its dramatic impact on the expression of the reporter apoaequorin, amiloride treatment did not induce toxic side effects and was able to correct the trafficking defect of all channel mutants tested. Interestingly, all amiloride derivatives were classified as active, and those with higher molecular weight reached FC_{max} at much lower concentrations (e.g., 2,4-dichlorbenzamil at 1 μM) (Supplemental Fig. 4). Nisoldipine and JFD03311 both caused an increase in apoaequorin expression in Western blot experiments, but only the effect of nisoldipine, and not JFD03311, was shown to impact the bioassay measurements (Fig. 4). Also, the effect of nisoldipine on other trafficking-deficient channels was inconsistent, whereas JFD03311 was able to increase surface expression of analyzed CNGA3 channels with mutations in the S4 region or the pore-forming region. Therefore, we conclude that ZD7288, the pyrazin amides and benzamides, and the DHP including JFD03311 may represent interesting starting points, supporting the development of therapeutics for trafficking-deficient CNGA3 channels.

Acknowledgments

We thank Dr. Charlotta Schärfe and Dr. Oliver Kohlbacher from the Center for Bioinformatics in Tübingen for their help regarding the selection of additional dihydropyridine compounds for the analysis of structural features important for the interaction with $CNGA3_{E228K}$. We also thank Dr. Hubert Kalbacher for technical advice and suggestions on protein analytics.

Authorship Contributions

Participated in research design: Wissinger, Kohl, Reuter.
Conducted experiments: Täger.
Performed data analysis: Täger, Reuter.
Wrote or contributed to the writing of the manuscript: Täger, Wissinger, Kohl, Reuter.

References

Adams BM, Oster ME, and Hebert DN (2019) Protein quality control in the endoplasmic reticulum. *Protein J* **38**:317–329.
Arduino DM, Wettmarshausen J, Vais H, Navas-Navarro P, Cheng Y, Leimpek A, Ma Z, Delrio-Lorenzo A, Giordano A, Garcia-Perez C, et al. (2017) Systematic identification of MCU modulators by orthogonal interspecies chemical screening. *Mol Cell* **67**:711–723.e7.
Atzmon A, Herrero M, Sharet-Eshed R, Gilad Y, Senderowitz H, and Elroy-Stein O (2018) Drug screening identifies sigma-1-receptor as a target for the therapy of VWM leukodystrophy. *Front Mol Neurosci* **11**:336.
Banning A, Gülec C, Rouvinen J, Gray SJ, and Tikkanen R (2016) Identification of small molecule compounds for pharmacological chaperone therapy of aspartylglucosaminuria. *Sci Rep* **6**:37583.
Blom TS, Linder MD, Snow K, Pihko H, Hess MW, Jokitalo E, Veckman V, Syvänen AC, and Ikonen E (2003) Defective endocytic trafficking of NPC1 and NPC2 underlying infantile Niemann-Pick type C disease. *Hum Mol Genet* **12**:257–272.
Brini M (2008) Calcium-sensitive photoproteins. *Methods* **46**:160–166.
Catterall WA and Swanson TM (2015) Structural basis for pharmacology of voltage-gated sodium and calcium channels. *Mol Pharmacol* **88**:141–150.
Chang B, Grau T, Dangel S, Hurd R, Jurklies B, Sener EC, Andreasson S, Dollfus H, Baumann B, Bolz S, et al. (2009) A homologous genetic basis of the murine cpfl1 mutant and human achromatopsia linked to mutations in the PDE6C gene. *Proc Natl Acad Sci USA* **106**:19581–19586.
Choo-Kang LR and Zeitlin PL (2001) Induction of HSP70 promotes DeltaF508 CFTR trafficking. *Am J Physiol Lung Cell Mol Physiol* **281**:L58–L68.
Conn PM and Janovick JA (2009) Drug development and the cellular quality control system. *Trends Pharmacol Sci* **30**:228–233.
Dandage R, Bandyopadhyay A, Jayaraj GG, Saxena K, Dalal V, Das A, and Chakraborty K (2015) Classification of chemical chaperones based on their effect on protein folding landscapes. *ACS Chem Biol* **10**:813–820.
Dawson G, Schroeder C, and Dawson PE (2010) Palmitoyl:protein thioesterase (PPT1) inhibitors can act as pharmacological chaperones in infantile Batten disease. *Biochem Biophys Res Commun* **395**:66–69.
Diamant S, Eliahu N, Rosenthal D, and Goloubinoff P (2001) Chemical chaperones regulate molecular chaperones in vitro and in cells under combined salt and heat stresses. *J Biol Chem* **276**:39586–39591.
Ding XQ, Fitzgerald JB, Quiambao AB, Harry CS, and Malykhina AP (2010) Molecular pathogenesis of achromatopsia associated with mutations in the cone cyclic nucleotide-gated channel CNGA3 subunit. *Adv Exp Med Biol* **664**:245–253.
Duricka DL, Brown RL, and Varnum MD (2012) Defective trafficking of cone photoreceptor CNG channels induces the unfolded protein response and ER-stress-associated cell death. *Biochem J* **441**:685–696.
Faillace MP, Bernabeu RO, and Korenbrot JI (2004) Cellular processing of cone photoreceptor cyclic GMP-gated ion channels: a role for the S4 structural motif. *J Biol Chem* **279**:22643–22653.
Gelsthorpe ME, Baumann N, Millard E, Gale SE, Langmade SJ, Schaffer JE, and Ory DS (2008) Niemann-Pick type C1 I1061T mutant encodes a functional protein that is selected for endoplasmic reticulum-associated degradation due to protein misfolding. *J Biol Chem* **283**: 8229–8236.
Gilberg E, Jasial S, Stumpfe D, Dimova D, and Bajorath J (2016) Highly promiscuous small molecules from biological screening assays include many Pan-assay interference compounds but also candidates for Polypharmacology. *J Med Chem* **59**:10285–10290.
Haq N, Grose D, Ward E, Chiu O, Tigue N, Dowell SJ, Powell AJ, and Chen MX (2013) A high-throughput assay for connexin 43 (Cx43, GJA1) gap junctions using codon-optimized aequorin. *Assay Drug Dev Technol* **11**:93–100.
Horvath P, Aulner N, Bickle M, Davies AM, Nery ED, Ebner D, Montoya MC, Östling P, Pietiäinen V, Price LS, et al. (2016) Screening out irrelevant cell-based models of disease. *Nat Rev Drug Discov* **15**:751–769.
Hoshina H, Shimada Y, Higuchi T, Kobayashi H, Ida H, and Ohashi T (2018) Chaperone effect of sulfated disaccharide from heparin on mutant iduronate-2-sulfatase in mucopolysaccharidosis type II. *Mol Genet Metab* **123**:118–122.

Jasial S, Hu Y, and Bajorath J (2017) How Frequently are Pan-assay interference compounds active? Large-scale analysis of screening data reveals diverse activity profiles, low global hit frequency, and many consistently inactive compounds. *J Med Chem* **60**:3879–3886.

Johnson S, Michaelides M, Aligianis IA, Ainsworth JR, Mollon JD, Maher ER, Moore AT, and Hunt DM (2004) Achromatopsia caused by novel mutations in both CNGA3 and CNGB3. *J Med Genet* **41**:e20.

Kamiya K, Niwa R, Morishima M, Honjo H, and Sanguinetti MC (2008) Molecular determinants of hERG channel block by terfenadine and cisapride. *J Pharmacol Sci* **108**:301–307.

Kaupp UB and Seifert R (2002) Cyclic nucleotide-gated ion channels. *Physiol Rev* **82**: 769–824.

Koeppen K, Reuter P, Kohl S, Baumann B, Ladewig T, and Wissinger B (2008) Functional analysis of human CNGA3 mutations associated with colour blindness suggests impaired surface expression of channel mutants A3(R427C) and A3(R563C). *Eur J Neurosci* **27**:2391–2401.

Koeppen K, Reuter P, Ladewig T, Kohl S, Baumann B, Jacobson SG, Plomp AS, Hamel CP, Janecke AR, and Wissinger B (2010) Dissecting the pathogenic mechanisms of mutations in the pore region of the human cone photoreceptor cyclic nucleotide-gated channel. *Hum Mutat* **31**:830–839.

Kohl S, Baumann B, Broghammer M, Jägle H, Sieving P, Kellner U, Spegal R, Anastasi M, Zrenner E, Sharpe LT, et al. (2000) Mutations in the CNGB3 gene encoding the beta-subunit of the cone photoreceptor cGMP-gated channel are responsible for achromatopsia (ACHM3) linked to chromosome 8q21. *Hum Mol Genet* **9**:2107–2116.

Kohl S, Baumann B, Rosenberg T, Kellner U, Lorenz B, Vadalà M, Jacobson SG, and Wissinger B (2002) Mutations in the cone photoreceptor G-protein α-subunit gene GNAT2 in patients with achromatopsia. *Am J Hum Genet* **71**:422–425.

Kohl S, Coppieters F, Meire F, Schaich S, Roosing S, Brennenstuhl C, Bolz S, van Genderen MM, Riemslag FCC, Lukowski R, et al.; European Retinal Disease Consortium (2012) A nonsense mutation in PDE6H causes autosomal-recessive incomplete achromatopsia. *Am J Hum Genet* **91**:527–532.

Kohl S, Marx T, Giddings I, Jägle H, Jacobson SG, Apfelstedt-Sylla E, Zrenner E, Sharpe LT, and Wissinger B (1998) Total colourblindness is caused by mutations in the gene encoding the alpha-subunit of the cone photoreceptor cGMP-gated cation channel. *Nat Genet* **19**:257–259.

Kohl S, Zobor D, Chiang WC, Weisschuh N, Staller J, Gonzalez Menendez I, Chang S, Beck SC, Garcia Garrido M, Sothilingam V, et al. (2015) Mutations in the unfolded protein response regulator ATF6 cause the cone dysfunction disorder achromatopsia. *Nat Genet* **47**:757–765.

Kuech EM, Brogden G, and Naim HY (2016) Alterations in membrane trafficking and pathophysiological implications in lysosomal storage disorders. *Biochimie* **130**:152–162.

Leandro P and Gomes CM (2008) Protein misfolding in conformational disorders: rescue of folding defects and chemical chaperoning. *Mini Rev Med Chem* **8**:901–911.

Leidenheimer NJ and Ryder KG (2014) Pharmacological chaperoning: a primer on mechanism and pharmacology. *Pharmacol Res* **83**:10–19.

Li JG, Chiu J, Ramanjulu M, Blass BE, and Praticò D (2020) A pharmacological chaperone improves memory by reducing Aβ and tau neuropathology in a mouse model with plaques and tangles. *Mol Neurodegener* **15**:1.

Liu C and Varnum MD (2005) Functional consequences of progressive cone dystrophy-associated mutations in the human cone photoreceptor cyclic nucleotide-gated channel CNGA3 subunit. *Am J Physiol Cell Physiol* **289**:C187–C198.

Martin GM, Chen PC, Devaraneni P, and Shyng SL (2013) Pharmacological rescue of trafficking-impaired ATP-sensitive potassium channels. *Front Physiol* **4**:386.

Matveev AV, Fitzgerald JB, Xu J, Malykhina AP, Rodgers KK, and Ding XQ (2010) The disease-causing mutations in the carboxyl terminus of the cone cyclic nucleotide-gated channel CNGA3 subunit alter the local secondary structure and interfere with the channel active conformational change. *Biochemistry* **49**:1628–1639.

Menon V, Ranganathn A, Jorgensen VH, Sabio M, Christoffersen CT, Uberti MA, Jones KA, and Babu PS (2008) Development of an aequorin luminescence calcium assay for high-throughput screening using a plate reader, the LumiLux. *Assay Drug Dev Technol* **6**:787–793.

Moura CS, Lollo PCB, Morato PN, and Amaya-Farfan J (2018) Dietary nutrients and bioactive substances modulate heat shock protein (HSP) expression: a review. *Nutrients* **10**:683.

Muraki-Oda S, Toyoda F, Okada A, Tanabe S, Yamade S, Ueyama H, Matsuura H, and Ohji M (2007) Functional analysis of rod monochromacy-associated missense mutations in the CNGA3 subunit of the cone photoreceptor cGMP-gated channel. *Bioche Biophy Res Commun* **362**:88–93.

Nakayama H and Kuniyasu A (1996) Identification of binding sites for calcium channel antagonists. *Jpn Heart J* **37**:643–650.

Nishiguchi KM, Sandberg MA, Gorji N, Berson EL, and Dryja TP (2005) Cone cGMP-gated channel mutations and clinical findings in patients with achromatopsia, macular degeneration, and other hereditary cone diseases. *Hum Mutat* **25**:248–258.

Nühs A, De Rycker M, Manthri S, Comer E, Scherer CA, Schreiber SL, Ioset JR, and Gray DW (2015) Development and validation of a novel leishmania donovani screening cascade for high-throughput screening using a novel axenic assay with high predictivity of leishmanicidal intracellular activity. *PLoS Negl Trop Dis* **9**:e0004094.

Patel KA, Bartoli KM, Fandino RA, Ngatchou AN, Woch G, Carey J, and Tanaka JC (2005) Transmembrane S1 mutations in CNGA3 from achromatopsia 2 patients cause loss of function and impaired cellular trafficking of the cone CNG channel. *Invest Ophthalmol Vis Sci* **46**:2282–2290.

Pedemonte N, Boido D, Moran O, Giampieri M, Mazzei M, Ravazzolo R, and Galietta LJV (2007) Structure-activity relationship of 1,4-dihydropyridines as potentiators of the cystic fibrosis transmembrane conductance regulator chloride channel. *Mol Pharmacol* **72**:197–207.

Remmer MH, Rastogi N, Ranka MP, and Ceisler EJ (2015) Achromatopsia: a review. *Curr Opin Ophthalmol* **26**:333–340.

Reuter P, Koeppen K, Ladewig T, Kohl S, Baumann B, and Wissinger B; Achromatopsia Clinical Study Group (2008) Mutations in CNGA3 impair trafficking or function of cone cyclic nucleotide-gated channels, resulting in achromatopsia. *Hum Mutat* **29**:1228–1236.

Rigat B and Mahuran D (2009) Diltiazem, a L-type Ca(2+) channel blocker, also acts as a pharmacological chaperone in Gaucher patient cells. *Mol Genet Metab* **96**:225–232.

Sato A, Arimura T, Makita N, Ishikawa T, Aizawa Y, Ushinohama H, Aizawa Y, and Kimura A (2009) Novel mechanisms of trafficking defect caused by KCNQ1 mutations found in long QT syndrome. *J Biol Chem* **284**:35122–35133.

Schaeffer C, Creatore A, and Rampoldi L (2014) Protein trafficking defects in inherited kidney diseases. *Nephrol Dial Transplant* **29** (Suppl 4):iv33–iv44.

Schild L, Schneeberger E, Gautschi I, and Firsov D (1997) Identification of amino acid residues in the α, β, and γ subunits of the epithelial sodium channel (ENaC) involved in amiloride block and ion permeation. *J Gen Physiol* **109**:15–26.

Shaikh RS, Reuter P, Sisk RA, Kausar T, Shahzad M, Maqsood MI, Yousif A, Ali M, Riazuddin S, Wissinger B, et al. (2015) Homozygous missense variant in the human CNGA3 channel causes cone-rod dystrophy. *Eur J Hum Genet* **23**:473–480.

Shuart NG, Haitin Y, Camp SS, Black KD, and Zagotta WN (2011) Molecular mechanism for 3:1 subunit stoichiometry of rod cyclic nucleotide-gated ion channels. *Nat Commun* **2**:457.

Skach WR (2000) Defects in processing and trafficking of the cystic fibrosis transmembrane conductance regulator. *Kidney Int* **57**:825–831.

Stevens M, Abdeen S, Salim N, Ray AM, Washburn A, Chitre S, Sivinski J, Park Y, Hoang QQ, Chapman E, et al. (2019) HSP60/10 chaperonin systems are inhibited by a variety of approved drugs, natural products, and known bioactive molecules. *Bioorg Med Chem Lett* **29**:1106–1112.

Täger J, Kohl S, Birch DG, Wheaton DKH, Wissinger B, and Reuter P (2018) An early nonsense mutation facilitates the expression of a short isoform of CNGA3 by alternative translation initiation. *Exp Eye Res* **171**:48–53.

Tamarappoo BK and Verkman AS (1998) Defective aquaporin-2 trafficking in nephrogenic diabetes insipidus and correction by chemical chaperones. *J Clin Invest* **101**: 2257–2267.

Tanguay J, Callahan KM, and D'Avanzo N (2019) Characterization of drug binding within the HCN1 channel pore. *Sci Rep* **9**:465.

Tränkner D, Jägle H, Kohl S, Apfelstedt-Sylla E, Sharpe LT, Kaupp UB, Zrenner E, Seifert R, and Wissinger B (2004) Molecular basis of an inherited form of incomplete achromatopsia. *J Neurosci* **24**:138–147.

Wang XH, Wang HM, Zhao BL, Yu P, and Fan ZC (2014a) Rescue of defective MC4R cell-surface expression and signaling by a novel pharmacoperone Ipsen 17. *J Mol Endocrinol* **53**:17–29.

Wang YJ, Di XJ, and Mu TW (2014b) Using pharmacological chaperones to restore proteostasis. *Pharmacol Res* **83**:3–9.

Wu X, Katz E, Della Valle MC, Mascioli K, Flanagan JJ, Castelli JP, Schiffmann R, Boudes P, Lockhart DJ, Valenzano KJ, et al. (2011) A pharmacogenetic approach to identify mutant forms of α-galactosidase A that respond to a pharmacological chaperone for Fabry disease. *Hum Mutat* **32**:965–977.

Yam GHF, Zuber C, and Roth J (2005) A synthetic chaperone corrects the trafficking defect and disease phenotype in a protein misfolding disorder. *FASEB J* **19**:12–18.

Yamamoto T, Niwa S, Ohno S, Tokumasu M, Masuzawa Y, Nakanishi C, Nakajo A, Onishi T, Koganei H, Fujita S, et al. (2008) The structure-activity relationship study on 2-, 5-, and 6-position of the water soluble 1,4-dihydropyridine derivatives blocking N-type calcium channels. *Bioorg Med Chem Lett* **18**:4813–4816.

Young JC (2014) The role of the cytosolic HSP70 chaperone system in diseases caused by misfolding and aberrant trafficking of ion channels. *Dis Model Mech* **7**:319–329.

Address correspondence to: Dr. Peggy Reuter, Molecular Genetics Laboratory, Institute for Ophthalmic Research, University of Tübingen, Elfriede-Aulhorn-Strasse 5-7, 72076 Tübingen, Germany. E-mail: peggy.reuter@med.uni-tuebingen.de